Earth Planet. Sci. Lett. 671 (2025) 119690

Contents lists available at ScienceDirect

Earth and Planetary Science Letters

journal homepage: www.elsevier.com/locate/epsl

The role of submarine volcanism in atmospheric chemistry

M. Colombier [a,*], M. Bonifacie [b], M. Brenna [c], A. Burke [d], C. Cimarelli [a], S.J. Cronin [e], P. Delmelle [f], D.B. Dingwell [a], K-U. Hess [a], M. Huebsch [e], T. Kula [g], F. Latu'ila [g], Y. Lavallée [a], G.W. Mann [h,n], T.A. Mather [i], J. Paredes-Mariño [e], T. Plank [j], B. Scheu [a], Y-J Sun [d], Z. Taracsák [k], S. Tegtmeier [l], S. Thivet [m], M. Toohey [l], I. Ukstins [e], J. Wu [c]

[a] Department of Earth and Environmental Sciences, Ludwig-Maximilians-Universität München, Munich, Germany
[b] Université Paris Cité, Institut de Physique du Globe de Paris, UMR 7154 CNRS, F-75005 Paris, France
[c] Department of Geology, University of Otago, Dunedin, New Zealand
[d] School of Earth and Environmental Sciences, University of St Andrews, St Andrews, UK
[e] School of Environment, University of Auckland, Auckland, New Zealand
[f] Earth and Life Institute, UCLouvain, Louvain-la-Neuve, Belgium
[g] Tonga Geological Services, Nuku'alofa, Tonga
[h] School of Earth & Environment, University of Leeds, Leeds LS2 9JT, United Kingdom
[i] Department of Earth Sciences, University of Oxford, Oxford OX1 3AN, United Kingdom
[j] Lamont Doherty Earth Observatory, Columbia University, Palisades, NY 10964-8000, United States of America
[k] Department of Earth Sciences, University of Cambridge, Cambridge CB2 3EQ, United Kingdom
[l] University of Saskatchewan, Institute of Space and Atmospheric Studies, Saskatoon SK S7N 5E2, Canada
[m] Department of Earth Sciences, University of Geneva, Geneva, Switzerland
[n] UK National Centre for Atmospheric Science, University of Leeds, Leeds LS2 9JT, United Kingdom

ARTICLE INFO

Editor: Dr C. M. Petrone

Keywords:
Submarine eruptions
Volcanic ash
Sulfates
Halogens
Atmospheric chemistry
Climate response

ABSTRACT

Submarine volcanic eruptions can form subaerial plumes that reach the stratosphere. Despite this, the impact of submarine eruptions on climate remains unclear due to a lack of clear geological record, with the recent large-scale Hunga eruption on 15 January 2022 being considered as an isolated case. Here, we review the impact of submarine and subaerial volcanoes in island or coastal settings (i.e., near seawater) on volatile/aerosol loading in the stratosphere. Isotopic $\delta^{34}S$ signatures of the Hunga ash suggest that $CaSO_4$ salts on the ash surface are dominantly formed by the evaporation of seawater during the eruption. We infer that SO_2 scavenging on volcanic ash did not play a major role in the lower-than-expected SO_2 detected in the volcanic cloud. Chlorine isotopic compositions ($\delta^{37}Cl$) also argue in favor of a seawater-derived origin of the chlorides from ash leachates. Combining petrological, leachate, isotopic and thermal analysis data, we demonstrate a near-absence of halogen degassing from the Hunga magma prior to and during the eruption, and conclude that the chlorine and bromine contents of tropospheric and stratospheric volatile species very dominantly derive from seawater/sea salts. We generalize our findings to all submarine eruptions, and large-scale, non-submarine eruptions in island or coastal settings, and propose that these may commonly form volcanic clouds that incorporate seawater thereby leading to the injection of related components (water vapor, sea salts, halogens) into the stratosphere. This makes seawater inputs a serious consideration when evaluating the long-term impact of volcanoes on climate.

1. Introduction

Explosive volcanism is responsible for the release of immense quantities of volcanic ash and gas (H_2O, CO_2, sulfur, halogens, etc.) into the atmosphere (Marshall et al., 2022). Recently, it has been realized that very substantial contributions to this atmospheric input may have their origins in the hydrosphere (e.g., Khaykin et al., 2022; Colombier et al., 2023; Wu et al., 2025). Such volcanic contributions, dispersed in the stratosphere, can seriously impact climate (e.g., Robock, 2000; Schmidt et al., 2012). Subaerial volcanism is dominant in observational

* Corresponding author at: Department für Geo- und Umweltwissenschaften, Sektion Mineralogie, Petrologie und Geochemie, Theresienstr. 41, 80333 München, Germany.
E-mail address: mathieu.colombier@min.uni-muenchen.de (M. Colombier).

https://doi.org/10.1016/j.epsl.2025.119690
Received 17 March 2025; Received in revised form 8 October 2025; Accepted 12 October 2025
Available online 18 October 2025

records relating to climate. While > 70 % of volcanism is submarine (Carey et al., 2018), much of this is deep (e.g., at mid-ocean ridges). Large-magnitude shallow submarine explosive eruptions certainly impacted the stratosphere in the past (Cronin, 1971; Prata et al., 2020; Carn et al., 2022), but the dearth of data on this event type during the satellite period has hindered evaluation of their climatic impact. The 15 January 2022 eruption of Hunga volcano (often referred to as Hunga Tonga-Hunga Ha'apai, the name of the emerging tuff cone formed during the 2014–15 eruption; Kingdom of Tonga) is thus a pivotal testbed to gain new insights into this interesting type of eruption.

The climate impacts of volcanic eruptions are strongly influenced by (1) plume elevation, (2) volcanic latitude, (3) season and (4) sulfur emissions (Robock, 2000; Timmreck, 2012). At high elevation in the stratosphere, volcanic products have long residence times up to several years (Marshall et al., 2022). They influence the climate by: (i) sulfate aerosols and ash particles impacting the radiative budget by back-scattering of incoming solar radiation and absorption of terrestrial infrared radiation, usually causing net warming of the stratosphere and cooling of Earth's surface (Robock, 2000), (ii) sulfate aerosols, NO_x and halogens reacting to cause ozone destruction (Krüger et al., 2015) and (iii) atmospheric circulation changes, e.g., leading to winter warming of Northern Hemisphere continents (e.g., Robock, 2000; Timmreck, 2012). Additional effects include anomalies in the stratospheric wind field and the global hydrological cycle (Robock, 2000). The temporal impact on climate was commonly assumed to be on the order of up to 1–2 years for a single large eruption (Robock, 2000). The impacts appear to last longer, up to a decade, in the cases of volcanic introduction of seawater into the atmosphere (Joshi and Jones, 2009; Zhou et al., 2024). In addition, stratospheric water vapor is expected to cause an opposite climate forcing compared to SO_2- and sulfate-rich subaerial eruptions, by promoting radiative cooling in the stratosphere and net warming in the troposphere (Sellitto et al., 2022).

Shallow (generally <500 m water depth) submarine eruptions can breach the sea surface (e.g., Cahalan and Dufek, 2021) and lead to efficient injection of water vapor into the atmosphere and stratosphere (Cronin, 1971). The Hunga 2022 event was the first eruption in the satellite era with a plume that reached the lower mesosphere at an altitude of 57 km. Total plume water load from this event was likely to be several thousand teragrams, with an output of 2880 Tg estimated only for the peak hour of plume growth (Mastin et al., 2024**).** Based on a new volatile budget, only ~319 Tg of magmatic water was released by the eruption, so that >90 % of the plume water content originated from seawater (Wu et al., 2025). Based on thermodynamic modelling of the eruption plume, Mastin et al. (2024) show that seawater mainly entered the plume as vapor. Whether as vapor or adhering water films on particles, much entrained water in the plume was rapidly converted to ice to generate the largest natural lightning event ever recorded (Van Eaton et al., 2023). In addition, much water vapor was directly injected into the stratosphere and mesosphere (150 Tg; Sellitto et al., 2022). Khaykin et al. (2022) proposed that this water had a strongly seawater-derived deuterium isotopic signature. Numerous spaceborne studies and climate models have investigated the unusual stratospheric aerosol burden associated with this eruption (e.g., Li et al., 2023; Millán et al., 2022; Sellito et al., 2022); yet, the influence of the submarine processes on aerosols (and other chemical constituents) was mostly neglected. For instance, the input of seawater, sea salts and marine-derived volatiles in the atmosphere/stratosphere and their resulting chemical and microphysical impact remain overlooked.

Interpretations of microphysical and chemical phenomena in the Hunga volcanic cloud in the aftermath of the eruption have been impacted by the comparison with other recent large magnitude subaerial eruptions, such as the 1991 Pinatubo eruption, or the 1982 El Chichón eruption (involving uptake of volatiles, fluids and salts from a hydrothermal system). The differences in (i) salt and volatile sources, (ii) fragmentation mechanisms (i.e., magmatic vs. hydrovolcanic, controlling the efficiency of fine ash generation) and (iii) amount of external water involved must be considered and systematically quantified to resolve the impact of aerosol and gas loading onto the atmosphere for these contrasting settings.

We contribute to this analysis by elucidating the aerosol and volatile budget associated with magma-seawater interaction during the 15 January 2022 Hunga eruption, based on chemical and thermal analysis of a unique fresh suite of volcanic ash samples. We also examine the frequency and potential impact of submarine-sourced eruption plumes that breach the tropopause. Finally, we discuss the impact of external salt and water sources in a range of volcanic settings on the atmospheric and climate response.

2. Methods

Samples HT1, HT6, HT7, HT8 and HT9 used for isotopic composition, as well as HT10 used for thermal analysis, correspond to ash deposits that were promptly collected after the eruption from different Tonga islands, with limited to no exposure to rain water after deposition (Colombier et al., 2023). HT6 also contains minor contamination with foreign material including rock, gravel, and calcareous sand (Colombier et al., 2023). The reader is referred to Colombier et al. (2023) for a detailed description of these samples and their collection.

2.1. Thermal analysis

Volatile content of the Hunga ash (sample HT10) was determined by evolved gas analysis (EGA) at the Ludwig-Maximilians-Universität (Germany) on a Mettler-Toledo TGA–DSC 3 + attached to a Pfeiffer Vacuum GSD 320 gas mass spectrometer on three types of coarse ash particles: (i) a dense glassy ash with a low degree of syn-eruptive degassing, (ii) a light-colored pumice with high vesicularity reflecting syn-eruptive degassing and (iii) a dark pumice with characteristics between dense glass and pumice (Fig. 1; Table SM1). Salts were removed from the surface of these particles by washing several times in distilled water. The cleaned particles were crushed and only the glassiest chips without visible phenocrysts were selected for thermal treatment. Ash fragments were heated in nitrogen atmosphere in two steps, first at a rate of 5 °C/min from 30 to 150 °C for dehydration and then at a rate of 30 °C/min from 150 °C to 1300 °C. More details on the methods are provided in Thivet et al. (2023) and Colombier et al. (2023).

2.2. Ash leachate database

We compiled leachate data from the literature on volcanic ash concentrations of Na^+, Cl^-, Ca^{2+}, SO_4^{2-}, Br^- and F^-. This database contains datasets obtained at 23 volcanoes worldwide, and also the composition of two crater lake waters/salts (Fig. 2; Table SM2 and references therein).

2.3. Sulfur isotope ratios, major element, and Cl contents in the melt inclusions

To estimate the sulfur isotopic composition of the melt feeding the 2022 Hunga eruption, we carried out $\delta^{34}S$ microanalyses on sample HT1 (Fig. 3; Table SM3). Sulfur isotope analyses were collected from volcanic glasses (mainly melt inclusions, MIs) hosted in clinopyroxene, orthopyroxene, and plagioclase using a CAMECA IMS-1280 secondary ion mass spectrometer (SIMS) at the Northeast National Ion Microprobe Facility, Woods Hole Oceanographic Institution. Analytical conditions during the $^{34}S/^{32}S$ analyses were identical to those described by Caliro et al. (2025). This included the analysis of $^{32}S^-$ and $^{34}S^-$ ions in multi-collection mode using a ~440 pA Cs^+ primary beam. Three glasses with known $\delta^{34}S$ compositions (Taracsák et al., 2021) were mounted alongside the Hunga samples and analyzed during the same session: A36 (Icelandic basalt), EGT17–01 (Canary Islands tephrite) and LIP-17,714 (Lipari obsidian). These glasses were mounted alongside the

unknowns. Standard deviation measured on glass A36 was 0.7‰ (1σ); considering all three standards analytical precision is estimated at 1.1‰ (1σ). Internal precision of analyses varied from 0.6 to 1.2‰ (1 S.E.) due to the overall low S content of the glasses. S contents from the SIMS analyses were quantified using a linear regression fitted between the known S content of the standards and the measured $^{32}S^-/^{30}Si^-$ ratios (Caliro et al., 2025).

Major elements, S and Cl contents in glasses (n = 40) and melt inclusion host crystals were analyzed using a CAMECA SX-100 electron microprobe (EPMA) at the University of Cambridge. We used the same analytical conditions and calibration standards as described in Caliro et al. (2025). Fluorine contents in the glasses were all below detection limit (<300 ppm). Sulfur concentrations measured by EPMA and SIMS are within ± 80 ppm for 17 out of 18 analyses. All data are provided in the supplementary spreadsheets.

Using the sulfur isotope data collected via SIMS, we carried out forward modelling to estimate the $\delta^{34}S$ value of volcanic gas and melt produced for a given S concentration (Fig. 3a). For this, we assumed a magmatic temperature of 1000 °C and that degassing proceeds according to the reaction $S^{(2-)}_{melt} => SO_{2,\ gas}$, likely reflecting of a somewhat reduced and evolved arc magmatic system degassing sulfur at shallow depth. Using the equations presented in Marini et al. (2011):

$$1000\ln(\alpha_{gas\text{-}melt}) = SO_2/\sum S_{gas} * 1000\ln(\alpha_{SO2—H2S}) + S^{6+}/\sum S_{melt} * 1000\ln(\alpha_{S2\text{-}(melt)\text{-}S6+(melt)}) + 1000\ln(\alpha_{H2S\text{-}S2\text{-}(melt)}),$$

we calculated the gas-melt fractionation factor during degassing of 1.002.

2.4. Sulfur isotope composition in the ash leachates

A total of four ash samples (0.2–0.5 g; Table 1) were leached with deionized water in dilution ratios of 1:20 for one hour. The concentrations of the leachates were analyzed by ion chromatography using a *Metrohm* 930 Compact IC Flex at the St Andrews Isotope Geochemistry (STAiG) laboratory, University of St Andrews. Further steps were carried out in a Class 100 cleanroom, and distilled acid was used. An amount of 50 nmol of sulfate from each leachate was separated for sulfur isotope measurement. The sample was dried down and converted to chlorine form (4 mL of 0.06 M HCl) prior to column chemistry. Sample purification was carried out using the *ESI* prepFAST-MC autodilution system packed with *BioRad* AG1 × 8 anion-exchange resin (100–200 mesh) in a 2 mL Teflon column. For each sample, the column was first cleaned with 1.4 M HNO_3 (10 mL) and 1.2 M HCl (10 mL), followed by conditioning with 0.06 M HCl (10 mL). The sample was then loaded onto the column, and the matrix was washed out with MQ water (10 mL). Sulfur was eluted with 0.5 M HNO_3 (4 mL). After collection, the column was washed with 1.4 M HCl (10 mL) and MQ water (10 mL) before the column cleaning step for the next sample. The column yield was greater than 95 %, and the procedural blank was <5 nmol for sulfur. Next, the samples were dried down and the appropriate amount of NaOH was added to the sample to matrix-match the in-house Na_2SO_4 bracketing standard. Triple sulfur isotopes (^{32}S, ^{33}S, and ^{34}S) were measured using a *Thermo Scientific* Neptune Plus multicollector inductively coupled plasma mass spectrometer, equipped with a *CETAC* Aridus II desolvation system. The precision and external reproducibility of isotope measurements were monitored with an in-house consistency standard. The results of this study fell within the long-term reproducibility (Switzer Falls river-water standard, $\delta^{34}S$ = 4.16 ± 0.06‰ and $\Delta^{33}S$ = 0.01 ± 0.05‰ V-CDT [Vienna–Canyon Diablo Troilite], 1SD; Burke et al., 2023).

Table 1
Sulfur isotope composition in the ash leachates from the 15 January 2022 Hunga eruption.

Sample number	$\delta^{34}S$	2*SD	$\delta^{33}S$	2*SD	$\Delta^{33}S$	2*SD
HT1	17.34	0.10	8.92	0.10	0.02	0.10
HT6	18.39	0.10	9.48	0.10	0.05	0.10
HT8	17.25	0.10	8.90	0.10	0.05	0.10
HT9	17.54	0.10	9.06	0.10	0.06	0.10

2.5. Chlorine isotopes in the ash leachates

The determination of chlorine isotopic compositions ($\delta^{37}Cl$) was performed at the Institut de Physique du Globe de Paris (IPGP) on two consecutive leaching steps (A and B in Table 2) of four Hunga ash samples: HT6, HT7, HT8 and HT9.

Each leaching step involves mixing approximately 1 *g* of ash sample in 4 mL of deionized water (milli-Q grade 18 mΩ), and ultrasonicating for 20 min before centrifuging (4000 tr/min for 5 min) to separate the leached powder and the supernatant leachate. Following collection of the first leachate, the remaining powder sample was passed through the same process again. The sample HT9 was fully run twice (#1 and #2 in Table 2) — i.e., a second batch of powder was independently leached two consecutive times (A and B).

The Cl isotopic composition for each leachate was determined following a routine procedure for $\delta^{37}Cl$ of chlorides in solution by dual-inlet measurements on gaseous CH_3Cl, based on the methods of Eggenkamp et al. (1994) and routinely used at IPGP (e.g., Bonifacie et al., 2005; Eggenkamp et al., 2016; Le Glas et al., 2025). The measurements of internal seawater standards in the same session (typical unknown:standard ratios of 3:1) allows $^{37}Cl/^{35}Cl$ ratios to be normalized as $\delta^{37}Cl$ values (in per mil, relative to SMOC - Standard Mean Oceanic chloride), and checked with five aliquots of the international reference material ISL-354. We found $\delta^{37}Cl$ = 0.03 ± 0.02‰ (1SD, n = 5) for ISL-354 salt, which is indistinguishable from the expected value. The long-term external reproducibility of $\delta^{37}Cl$ values at IPGP is lower than ±0.04‰ (1 SD) evaluated on independent replicates of the whole procedure on our internal seawater standard Atlantique 2 (n > 150), and also checked on ten seawater analyses run over the course of this study.

2.6. Catalogue of stratospheric injections of volcanic clouds following submarine and crater lake eruptions

We collated published studies of volcanic eruptive clouds formed during submarine eruptions that breached the tropopause (Table SM4

Table 2
Chlorine contents and isotopic compositions of ash leachates and reference materials used in this study. Total Cl contents and isotopic compositions obtained in this study are given in bold fonts for each couple of consecutive leachates (A + B). The Cl content values in parentheses are those reported on Colombier et al. (2023). "Fraction" represents the proportion of Cl extracted in the leachate relative to the total amount of Cl extracted for a given sample.

Sample	[Cl] ppm	Fraction (%)	$\delta^{37}Cl$ (‰, SMOC)
HT6 A	3497	92	0.189
HT6 B	305	8	0.210
	3802 *(3600)*		***0.200*** ± ***0.015*** ‰
HT7 A	5406	87	0.147
HT7 B	806	13	0.129
	6212		***0.138*** ± ***0.013*** ‰
HT8 A	2694	92	0.010
HT8 B	248	8	0.010
	2942 *(2800)*		***0.010*** ± ***0.00*** ‰
HT9#1 A	9748	88	0.011
HT9#1 B	1379	12	0.006
	11127 *(11000)*		***0.009*** ± ***0.004*** ‰
HT9#2 A	10,148	87	−0.023
			−0.034
HT9#2 B	1534	13	−0.011
			0.007
	11681 *(11000)*		***−0.015*** ± ***0.018*** ‰
Reference seawater (n = 10)			***0.002*** ± ***0.013*** ‰
ISL354 (n = 5)			***0.028*** ± ***0.020*** ‰

and references therein). Information on plume height for submarine eruptions is more commonly found in the literature since the shallow submarine Surtsey 1963 eruption where stratospheric injection was first observed. The reported height of the tropopause was used when available. When it was not reported, we used the profile of tropopause height variation with latitude from Cronin (1971). In cases where the plume is mentioned to have entered the stratosphere without specifying the height, we report the tropopause height as a minimum estimate. In several cases the plume spread when it encountered the tropopause, so the plume height is very close to the tropopause.

3. Results

3.1. Sulfur and halogen degassing during heating of the Hunga ash

Fig. 1 shows the degassing of volatile species (H_2O, CO_2, SO_2 and HCl) below and above the glass transition temperature (T_g) during reheating of the Hunga ash. For dense glass, light and dark pumice, we observed a magmatic release of H_2O and CO_2 at $T>T_g$, with a minor amount of SO_2 degassing. We note that H_2S was not detected during the analysis. There is an absence of HCl degassing below 1300 °C (>30 % higher than the eruptive temperature).

3.2. Ash leachate compilation

Leachates of Hunga salt-ash mixtures from the 2014–15 and the 2022 eruptions reveal unique features when compared to a global volcanic dataset for subaerial eruptions (Fig. 2). NaCl and $CaSO_4$ salts are frequently observed on volcanic ash at many volcanoes characterized by magmatic, crater lake and/or hydrothermal activity, and commonly show a 1:1 stoichiometric molar relationship. Compared to these data, Hunga ash is characterized by the tightest 1:1 molar trends for both these cation–anion pairs, and by the highest concentrations of NaCl (Fig. 2a,b). In addition, observed concentrations commonly fall near the seawater endmember and a seawater-ash mixing line (calculated by assuming complete transfer of ions from the seawater to ash particles during evaporation and varying the seawater-to-ash ratio). Br concentrations are also in agreement with seawater-ash mixing (Fig. 2c). Finally, the fluorine content is the lowest observed for such high Cl concentrations, and plots near the seawater endmember (Fig. 2d).

3.3. Isotopic measurements of volcanic glasses

Melt inclusions (MIs), embayments and matrix glasses analyzed for their major element, S, and Cl contents are basaltic andesitic to andesitic in composition, with plagioclase-hosted MI being the most evolved (higher SiO_2). Sufur contents of all glasses are between 190 and 850 ppm, while the Cl content range is 730–2550 ppm. The Cl/K ratio of most glasses (37 out of 41) is between 0.3 and 0.5; four plagioclase-hosted MI have higher Cl/K, reaching 0.85. The Cl/S ratios in glasses vary from 1.2 to 11, and correlates positively with Cl.

Measured $\delta^{34}S$ (n = 18) values in glasses is between −0.7‰ to +6.4‰, with more sulfur-rich glasses enriched in ^{34}S (Fig. 3a). Glass $\delta^{34}S$ values broadly increase with increasing MgO and decreasing SiO_2. Calculated degassing paths show decreasing $\delta^{34}S$ as the melt loses S to vapor, thus creating a gas phase with higher $\delta^{34}S$ than the melt. Parental melts with +3 to +7 per mil $\delta^{34}S$ decrease to +1 per mil after 77 % degassing of S, creating a bulk vapor with $\delta^{34}S$ of +4 to +8 per mil (Fig. 3a).

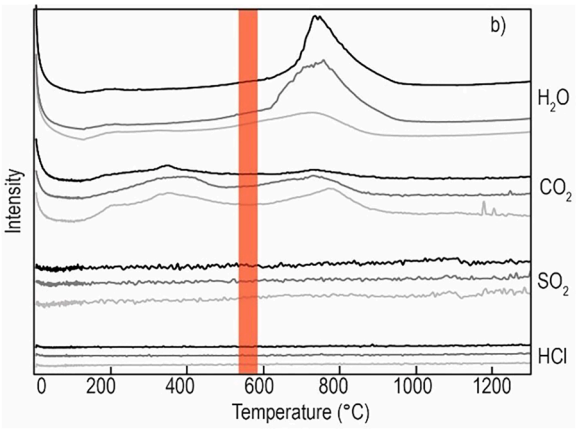

Fig 1. Evolved Gas analysis showing the degassing of volatile species (H_2O, CO_2, SO_2 and HCl) below and above the glass transition temperature (red area; Colombier et al., 2018) during reheating of the Hunga coarse ash (black: dense glass; dark grey: intermediate; light grey: pumice). Note the absence of HCl degassing up to 1300 °C.

3.4. Isotopic measurements in ash leachates

The Cl concentration was determined for each leaching step by quantification of CH_3Cl amount just before $\delta^{37}Cl$ measurements (Table 2). The total amount of Cl extracted yielded overall Cl contents between 2,842 and 11,681 ppm. In details, the proportion of Cl extracted over the first leachate is higher than 87 % compared to 13 % extracted during the second leachates. This indicates that most of chlorine from the sample is easily solubilized, most likely as chlorides. As importantly, though the leaching procedures used were different, the Cl contents found here are similar (i.e., not deviating by >5 % from each other) to those reported for the same samples in Colombier et al. (2023). This indicates that all the soluble Cl present in ash samples have been extracted as chlorides and analyzed for their $\delta^{37}Cl$ value. Noticeably, the fact that the HT9 sample shows similar results on the two batches ran also argues in favor of this hypothesis.

For the four samples, the differences between the $\delta^{37}Cl$ values found for the two consecutive leachates of the same powder are smaller than the long-term external reproducibility on $\delta^{37}Cl$ values at IPGP (± 0.04‰; 1 SD). This indicates that the sample is highly homogeneous for its Cl isotopic composition. The four analyzed samples show $\delta^{37}Cl$ values only varying little (between −0.015‰ and +0.200‰), and very close to that of seawater ($\delta^{37}Cl = 0$‰), with however a slight enrichment in HT6 and HT7.

We found elevated $\delta^{34}S$ values (17.25–18.39‰) in the ash leachates (Table 1).

4. Discussion

4.1. The sulfur budget during the 15 January 2022 Hunga eruption

For submarine eruptions of both Hunga (Tonga, 2022) and Anak Krakatau (Indonesia, 2019), the SO_2 concentration measured by satellites was orders of magnitude lower than expected given the size of the eruptions (Prata et al., 2020; Carn et al., 2022). At Hunga, the difference between MIs and glass (Fig. 3b) combined with the mass of erupted magma suggests 18.8 Tg of SO_2 from degassing (Wu et al., 2025) whereas only 0.6 Tg was measured by satellites (Carn et al., 2022). This value may be slightly underestimated due to the opacity of the early plume from ash/ice content as suggested by Sellitto et al. (2022) who proposed a SO_2 burden of 1Tg. Previous studies explained the discrepancies between the large magnitude of the eruption and the low SO_2 content by (i) gas scavenging by volcanic ash to form $CaSO_4$ (Prata et al., 2020; Colombier et al., 2023), (ii) passive outgassing to the sea prior to eruption or syn-eruptive emplacement in submarine density currents (Colombier et al., 2023; Wu et al., 2025) and (iii) faster conversion rates of SO_2 to sulfate aerosols due to water vapor injection (Sellitto et al., 2022; Legras et al., 2022). The latter process and formation of H_2SO_4 was estimated to be in the range of 1 to 3 Tg in early February 2022 (Sellitto et al., 2022) (corresponding to 0.65–1.96 Tg SO_2), which is

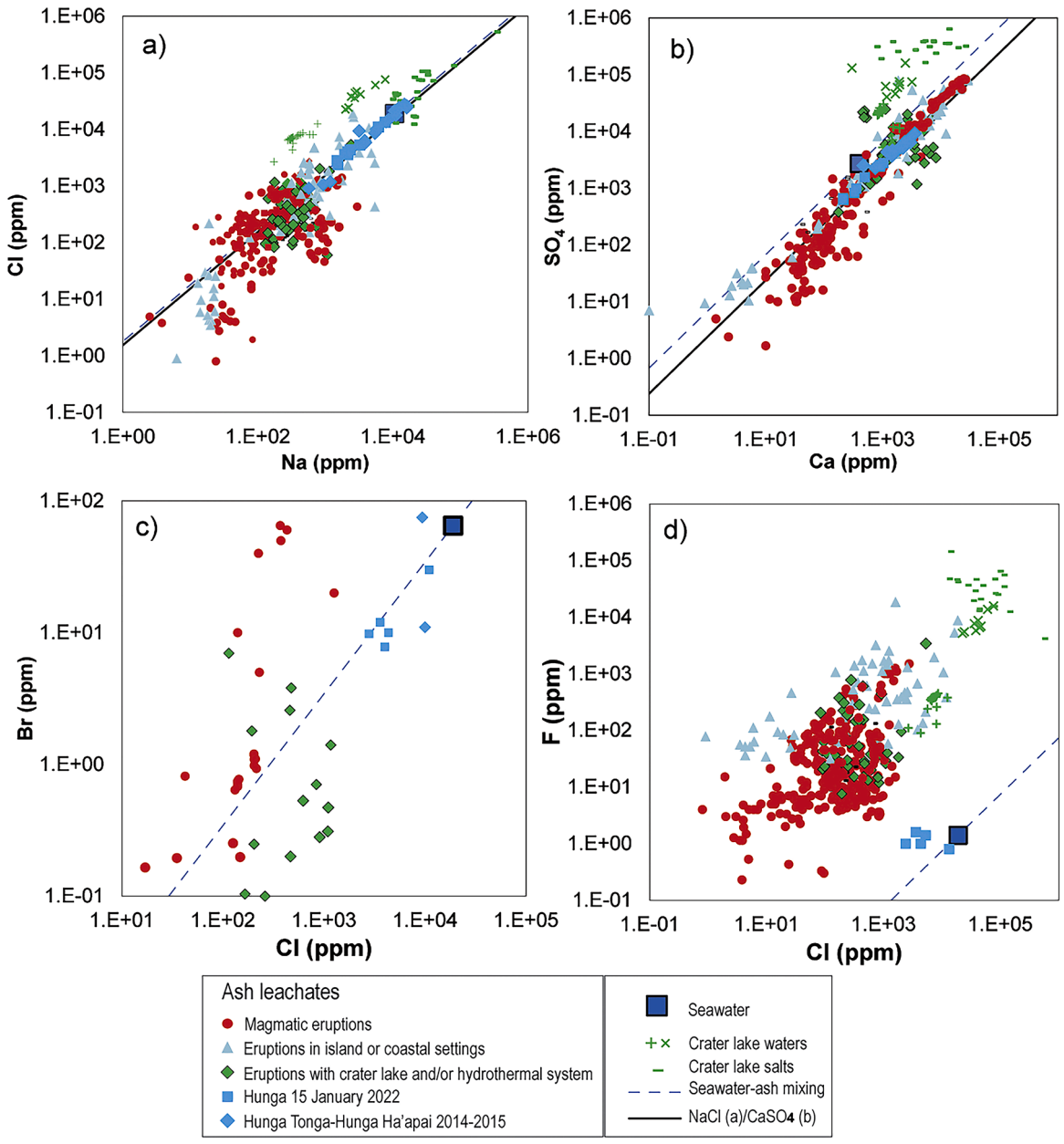

Fig 2. Compilation of ash leachate data (see table SM2 and references therein). Solid lines for NaCl (a) and $CaSO_4$ (b) represent stoichiometric 1:1 molar relationship. Magmatic eruptions refer to eruptions far away from a seawater source and with no reported evidence of crater lake nor hydrothermal system. Eruptions in island or coastal settings correspond to eruptions at volcanoes with a crater <2 km away from the sea/ocean.

insufficient to explain the observed discrepancy.

The formation of $CaSO_4$ by scavenging by volcanic ash has been used to explain the stoichiometric 1:1 molar relationship between Ca^{2+} and SO_4^{2-} in ash leachates (Fig. 2). It is also demonstrated in experiments exposing volcanic ash to SO_2 at high temperatures with optimal efficiency at 600–800 °C (Ayris et al., 2013). However, in the Hunga case seawater evaporation is an additional source for the formation of $CaSO_4$, which is dominantly present in a hydrated form of gypsum and/or bassanite (Colombier et al., 2019, 2023). Combining S isotopic data of the leachates and melt inclusions, we can calculate the fraction of $CaSO_4$ arising from the seawater source using the formula:

$$CaSO_{4\text{-seawater}} = (\delta^{34}S_{leachate} - \delta^{34}S_{magmatic}) / (\delta^{34}S_{seawater} - \delta^{34}S_{magmatic})$$

$\delta^{34}S_{magmatic}$ is the isotopic composition of the ash leachate sulfate that derives from magmatically degassed SO_2. There are several potential fractionation steps in estimating this isotopic value from that in the Hunga melt inclusions that we measured, including degassing SO_2 from mixed melt redox species, and then oxidation to form Ca-sulfate deposits on the ash surface. Despite some studies arguing for strong enrichment in ^{34}S in this process (Bindeman et al., 2007), we note that de Moor et al. (2010) find little fractionation between ash leachate $\delta^{34}S$ and degassed pumice $\delta^{34}S$ in the sub-aerial 2003 eruption of Anatahan volcano in the Marianas islands.

Rare sulfides were detected on the ash surfaces (Colombier et al., 2023). These sulfdes are likely hydrothermal in origin, as they are not part of the primary magmatic mineral assemblage (Wu et al., 2025). The sulfur isotopic composition of hydrothermal sulfides typically falls below 10 ‰, and is often negative (e.g., Rye, 1993; Arribas, 1995). Therefore, the presence of rare sulfides in the Hunga ash cannot account for the high $\delta^{34}S$ values measured in the leachates. The disproportionation-hydrolysis reaction of SO_2 gas in water can produce sulfate that is distinctly enriched in ^{34}S (Kusakabe et al., 2000). For

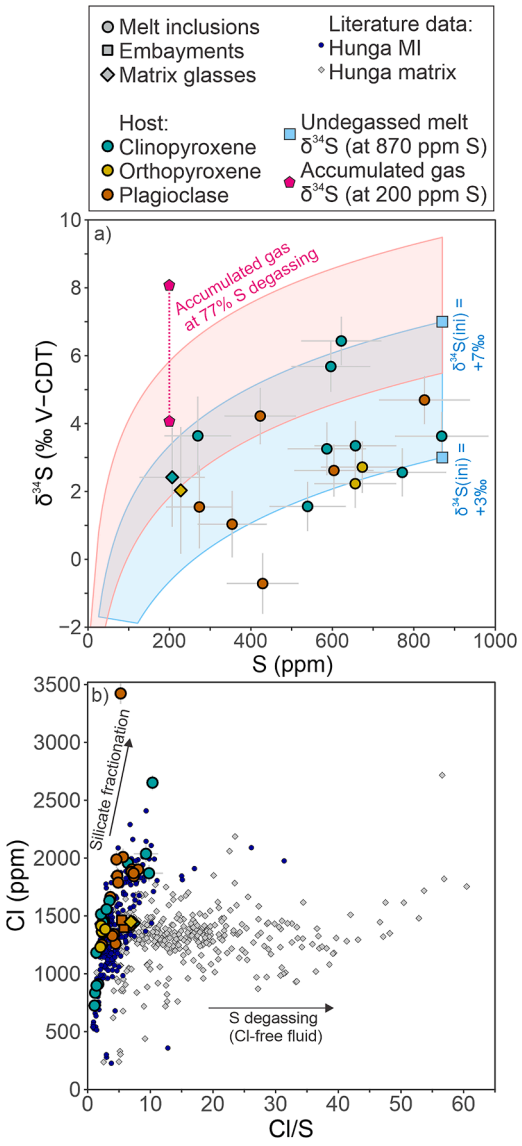

Fig 3. Sulfur isotope ratios plotted against S content (measured by SIMS) – in (a), Hunga 2022 data is shown alongside open system equilibrium degassing models: blue area show the melt, while the pink area shows the gas composition range. For the degassing models, initial $\delta^{34}S$ values were set at +3‰ and +7‰ (blue squares), while degassing was assumed to be driven by dissolved S^{2-} degassing as SO_2 at 1000 °C (fractionation factor at 1.0025). Accumulated gas $\delta^{34}S$ (at 200 ppm melt S content) is calculated at +8‰ and +4‰ for initial melt $\delta^{34}S$ values of +7‰ and +3‰, respectively (magenta pentagons). In (b), Cl contents against Cl/S ratios are shown, alongside literature glass data from the same eruption (Wu et al., 2025). Fractionation of silicates increases Cl contents at near constant Cl/S, while degassing of S alone would increase Cl/S at constant Cl content. Error bars are 1σ.

example, dissolved sulfate from hyper acid crater lakes receiving magmatic-hydrothermal fluids can exhibit $\delta^{34}S$ values approaching 20 ‰ (Delmelle and Bernard, 2015). Disproportionation of magmatic SO_2 in water-droplets could have occurred within the eruption plume, with the resulting isotopically heavy sulfate potentially contributing to the formation of Ca-sulfate deposits on the ash surface. However, this contribution was likely minor due to the substantial loss of magmatic SO_2 to the sea during subaqueous degassing.

If we assume Hunga $\delta^{34}S_{magmatic}$ is similar to the most degassed melt inclusions (~1 ‰ $\delta^{34}S$), and that seawater $\delta^{34}S$ is +21 ‰ $\delta^{34}S$, we calculate 85 % of the leachate sulfate (ave $\delta^{34}S$ of 18) as seawater-derived. This is a maximum value given that +1 ‰ is likely a minimum value for $\delta^{34}S_{magmatic}$. If instead $\delta^{34}S_{magmatic}$ is 8 ‰, similar to the total SO_2 evolved along the Hunga MI degassing path (Fig. 3a), then the seawater fraction is 77 %. Thus, despite the uncertainties in the magmatic gas composition, most (77–85 %) of the ash leachate sulfur is seawater-derived, and a minor amount magmatic (15–23 %). This isotope mass balance would be consistent with the submarine nature of the eruption and evidence for massive seawater entrainment in the plume, subsequent evaporation and significant sea salt precipitation (Colombier et al., 2023).

The total mass of $CaSO_4$ entrained in the plume can be obtained from the total mass of ash fallout and the leachate concentrations (620–2400 ppm of sulfate for samples collected before significant exposure to rainwater; Colombier et al., 2023). Taking this range and 1190 Tg of tephra ejected (Wu et al., 2025) yields around 0.74–2.86 Tg of sulfate (in the form of $CaSO_4$), with only 15–23 % (~0.11–0.66 Tg of sulfate) coming from magmatic gas scavenging. The corresponding SO_2 removal by gas scavenging and $CaSO_4$ precipitation would be only 0.05–0.31 Tg. Adding this missing SO_2 to the 0.6 Tg measured by satellites is still far from resolving the SO_2 discrepancy observed. Chemical scavenging of SO_2 by external water (vapor and/or ice) was a potential additional sink for sulfur in the plume (e.g., Rowell et al., 2022). However, it is likely that SO_2 was mainly lost by a combination of degassing to the sea prior to eruption and syn-eruptive emplacement in submarine density currents as recently proposed by Wu et al. (2025).

4.2. The source of halogens in the Hunga volcanic cloud

The atmospheric halogen signals of chlorine and bromine species in the Hunga 2022 volcanic cloud were initially interpreted as originating from magma degassing (Li et al., 2023; Santee et al., 2023). Evolved gas analysis revealed the absence of HCl degassing during reheating of the Hunga ash up to 1300 °C, at atmospheric pressure, suggesting that Cl measured in the glass was stable in the melt at eruptive temperatures (Fig. 1). An increase in Cl contents in MIs and glasses with decreasing MgO and S contents suggest Cl did not degas alongside S. Absence of HCl degassing is also supported by the petrological analysis of the Hunga ash, with similar Cl concentrations in the melt inclusions and the residual glass (Fig. 3b; Wu et al., 2025). F concentrations are below the detection limit (700 ppm at 3σ confidence) in both the melt inclusions and the residual glass, in agreement with published data (Wu et al., 2025). Chlorine, Br and F concentrations in the ash leachates suggest a submarine source, as concentrations are significantly different compared to other volcanoes dominated by degassing or interactions with crater lakes (Fig. 2). The absence of F and in contrast elevated Cl and Br concentrations, as well as the 1:1 stoichiometric trend for the Na-Cl molar concentrations, suggest a dominant process of halite precipitation during seawater-ash mixing (Fig. 2).

Although NaCl soluble salts can be formed by scavenging of magmatic HCl and uptake of Na from ash particles in a volcanic plume, this process can be ruled out at Hunga in favor of a seawater source for the Cl by (i) the absence of HCl degassing (Figs. 1 and 3), (ii) the NaCl trends that are enriched towards the seawater endmember and absence of 1:1 relationship for other volcanoes (Fig. 2) and (iii) the chlorine isotopic compositions of ash leachates which are close to the seawater value ($\delta^{37}Cl$ values near zero Table 2. We conclude that halogen volatiles detected by satellites in the Hunga plume (as HCl and BrO; e.g., Millán et al., 2022; Li et al., 2023; Colombier et al., 2023) did not originate from magma degassing but instead from sea salt precipitation during seawater evaporation. Cl and Br volatiles were likely formed by dehalogenation of these sea salts (Figs. 1, 2 and 3), as previously proposed by Colombier et al. (2023). For HCl, this process can, for instance, occur at an early stage in a water vapor-rich volcanic plume via the hydrolysis reaction (Edmonds and Gerlach, 2006):

$$NaCl + H_2O(gas) \rightarrow NaOH + HCl(gas) \quad (1)$$

Similar reactions may have taken place to form HBr species that were rapidly converted to oxidized forms such as BrO (Li et al., 2023; Colombier et al., 2023). HCl injection following the Hunga 2022 eruption was described as unexceptional, however the height of the injection was unique (Millán et al., 2022). This unexceptional HCl despite the scale of the Hunga event is likely a result of the negligibility of a magmatic component, and the prevalence of Cl- and Br-species that mostly remained as particulate matter and were not transformed to volatiles, as also observed during laze formation following lava-seawater interaction (Mason et al., 2021). In addition, scavenging of soluble gas by liquid/solid hydrometeors may have contributed to reduce HCl concentrations during transit through the lower atmosphere (e.g., Mather, 2015).

Despite the somewhat unexceptional nature of this injection, several studies have explained the unprecedented tropical ozone depletion rates during the Hunga 2022 eruption via the role of reactive halogen (Cl- and Br-bearing) species on heterogeneous reactions on sulfate aerosols (Zhu et al., 2023; Evan et al., 2023; Zhang et al., 2024).

4.3. Climatic impact of sea salts

It remains unclear how much of the long-lived sulfate aerosols residing in the Hunga stratospheric cloud derive from seawater. It is likely that the majority of sulfate aerosols arose from the conversion of magmatic SO_2 to H_2SO_4 (Sellito et al., 2024). But it is also plausible that sea-derived Ca-sulfates and NaCl were mixed with H_2SO_4 aerosols, fine ash and water vapor in the stratospheric cloud, potentially contributing to the anomalous radiative balance.

Based on previous estimates, >99.9 % of the sea salts injected in the Hunga plume were not transformed to a volatile halogen phase (Colombier et al., 2023; Zhu et al., 2023). These salts, present as particulate matter in the cloud, still exerted a strong control on the residence time of ash and aerosols in the atmosphere, and potentially the grain size of remaining aerosols in the stratosphere. Rapid removal of ash particles larger than 1 μm was discussed for the Hunga plume contrasting with other volcanic plumes formed following large-scale eruptions such as the Pinatubo 1991 eruption (Kloss et al., 2022; Gupta et al., 2022). Ash removal may be enhanced by interactions with ice particles (Gupta et al., 2022), although our previous observations suggest that a dominant mechanism is the coating of fine ash (here defined as particles of 1 μm up to several tens of μm) around coarse particles (coarse ash up to 2 mm in diameter or small lapilli) (Colombier et al., 2023). Previous experiments and analysis of submarine tephra revealed that the presence of NaCl and $CaSO_4$ salts efficiently promote ash aggregate stability (Mueller et al., 2017; Colombier et al., 2019) and therefore contribute to the rapid removal of fine to coarse ash from the volcanic plume. For the even finer particles (<1 μm) that remained in the stratospheric cloud, binding between ash and sea salts may have contributed to the specific aerosol optical properties and size distributions discussed by Baron et al. (2023) based on Lidar measurements in La Réunion one week after the eruption. Balloon measurement and sampling by Vernier et al. (2025) suggested the presence of NaCl sea salts in the stratosphere eight months after the eruption. Based on this observation, Zhu et al. (2023) proposed that most of the NaCl injected in the cloud was not converted to HCl but stayed as particulate matter in the stratosphere. Based on our leachate analyses, we believe that most of the NaCl was removed from the stratosphere rapidly by efficient binding with the volcanic ash forming aggregates, but that the finest particles remained in the stratospheric aerosol layer.

4.4. Submarine eruptions reaching the stratosphere

The fact that the highest NaCl contents are observed for the two submarine eruptions included in the leachate database (Fig. 2; 2014–15 and 2022 Hunga eruptions) suggests that this may be a distinguishing feature of any magnitude of explosive submarine eruption breaching the sea surface. Rose et al. (1995) proposed a similar scenario for seawater evaporation followed by precipitation and injection of sea salts into the stratosphere during the 1994 Vulcan cone eruption in Rabaul caldera (Papua New Guinea). Johnson and Threlfall (2023) reported a noticeable chlorine signature in the associated deposits and attributed it to the influence of seawater on the Rabaul phreatoplinian eruption.

The main features of large-scale submarine eruption columns reaching the stratosphere include: (1) low ash content dominated by fine ash particles; (2) a high water vapor content originating from seawater, and (3) high contents of sea-salt (Prata et al., 2020; Maeno et al., 2022; Colombier et al., 2023; Mastin et al., 2024). Stratospheric cooling observed in the weeks following the eruption at Anak Krakatau and Hunga may be an additional common feature of these eruptions (Prata et al., 2020; Sellitto et al., 2022). There exist several other similarities between atmospheric processes following the phreatoplinian phase of the Vulcan cone of the Rabaul caldera 1994 eruption, the 2018–19 Anak Krakatau Surtseyan phase and the Hunga 2022 submarine eruption. In all cases, a lower-than-expected SO_2 output was reported in relation to the magnitude of the event and/or magma chemistry (Rose et al., 1995; Prata et al., 2020; Carn et al., 2022; Colombier et al., 2023; Wu et al., 2025). In all cases a high water content caused substantive ice generation (Rose et al., 1995; Prata et al., 2020; Khaykin et al., 2022) and associated lightning (McNutt and Williams, 2010; Mckee et al., 2018; Prata et al., 2020; Yuen et al., 2022;Ichihara et al., 2023; Van Eaton et al., 2023). Lightning is promoted by the high ice content, but possibly augmented by salinity and very fine ash particles generated during magma-seawater interaction.

Submarine eruptions similar or larger in magnitude to the Hunga event likely occurred on several other occasions in the last millennia globally, although these records are likely highly incomplete (Mastin and Witter, 2000). Examples of similar shallow, submarine calderas include the Santorini-Kolumbo complex (Greece). The Minoan eruption of Santorini ~1470 BC. was a caldera-forming Plinian eruption involving extensive seawater-magma interaction (Bond and Sparks, 1976). The 1650 CE Kolumbo eruption was caldera-forming and breached the ocean surface, with an explosivity index of ~5 (Ulvrova et al., 2016). Many other shallow submarine volcanoes are poorly known and may (i) be the source of some large-scale unidentified eruptions in polar ice cores and historical records (Oppenheimmer, 2003) or (ii) have formed deposits that are absent from these records. In addition, we anticipate that a stratospheric impact of submarine eruptions can be associated with events far smaller than Hunga 2022, especially for events at polar latitudes (Cronin, 1971). Since the mildly explosive eruption of Surtsey in 1963, submarine eruption plumes reached the tropopause or stratosphere frequently (Fig. 4). Thus a global budget for the impacts of submarine eruptions must also include smaller scale events (e.g., Rabaul or Anak Krakatau).

4.5. Seawater and sea-salts during volcanic island and coastal eruptions

The 2022 Hunga event had comparable energy to the 1883 Krakatau eruption (Wright et al., 2022). The latter did not start as submarine event, but from a volcanic island. The initial climactic activity from Krakatau in 1883 included phreatomagmatic explosions (Verbeek, 1884; Self and Sparks, 1978; Camus and Vincent, 1983), but the highest plume altitude was reached after caldera collapse and was generated by pyroclastic density currents entering the sea (Self and Rampino, 1981; Self, 1992). These generated secondary co-ignimbrite plumes (Mandeville et al., 1998) and likely injected vaporized seawater high into the stratosphere at a similar scale to Hunga in 2022. At Krakatau excess H_2O burden to the stratosphere was estimated at 500Tg (Joshi and Jones, 2009). The Krakatau event was followed by widespread purple twilight observations in the tropics, indicating the aerosol descended from 32 km to 24 km in the first weeks post-eruption (Pernter et al., 1889; Wexler et al., 1951). The Hunga plume descent rate was remarkably similar (Sellitto et al., 2022; Legras et al., 2022), and

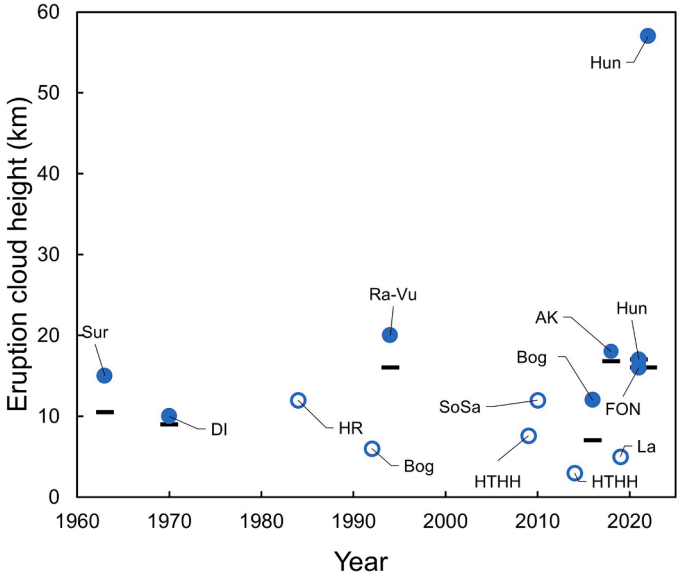

Fig 4. Frequency of stratospheric injections of submarine volcanic clouds since the 1963 Surtseyan eruption of Surtsey. Blue filled circles represent submarine with plume heights above the tropopause (represented by a black line), while open circles represent examples of submarine eruptions that only reached the troposphere. Sur: Surtsey; DI: Deception Island; HR: Home Reef; SoSa: South Sarigan; BOG: Bogoslof; Ra-Vu: Rabaul-Vulcan; AK: Anak Krakatau; FON: Fukutoku-Oka-noBa; HTHH- Hunga Tonga-Hunga Ha'apai; Hun: Hunga; See table SM4 and references therein.

consistent with strong radiative cooling from the emitted water vapor. In addition to Krakatau, other high magnitude eruptions from volcanic islands or coastal areas could readily remobilize seawater by pyroclastic flows (Joshi and Jones, 2009). Even small eruption-generated pyroclastic density currents interact with seawater to cause steam explosions and sea salt precipitation (e.g., Soufrière Hills volcano, Montserrat; Colombier et al., 2019), but the atmospheric impacts are limited to the troposphere.

Several eruptions showing stratospheric increases of HCl and H_2O (Fig. 3 in Millán et al., 2022), likely involved an external source of seawater vapor and sea salts. For instance, the Kasatochi and Raikoke volcanoes are <300 m from the coast and have salt-water affected ground waters (in one case a crater lake) (Grishin et al., 2021). Similar phreatomagmatic activity involving seawater readily produces high steam-rich plumes (e.g., Németh and Cronin, 2009). In addition, lava flows entering the sea produce Cl-rich plumes and laze (e.g., Mason et al., 2021), although likely confined to the troposphere. In other cases, volcanic plumes may interact with sea salt aerosols in the lower troposphere in marine environments (Murphy et al., 2019), as seen by increases in the chlorinity of rainwater up to tens of kilometers inland (Junge and Gustafson, 1957; Edmonds et al., 2003).

4.6. *Hydrothermal system salts*

Hydrothermal systems and crater lakes disturbed by eruptions may also provide large masses of water vapor and salts to volcanic plumes. This is especially noted for the 1982 El Chichón eruption (Mexico), the 1995–1996 eruption of Ruapehu (New Zealand) and the 2014 eruption of Aso volcano (Japan) (supplementary table SM2 and references therein). Ash leachates from these eruptions have unique salt assemblages, often including high F, Cl and S contents (Fig. 2). Other eruptions on glacier-capped volcanoes or those with large ground water reservoirs likely injected large volumes of water into the atmosphere, such as the Calbuco 2015 eruption (Sioris et al., 2016). These processes are generally overlooked in studies focused on the link between climate and volcanic activity.

5. Conclusion

The unique nature of the coupled seawater-magmatic sources for aerosols and volatiles injected in the atmosphere during submarine eruptions has distinct impact on atmospheric chemistry and climate compared to subaerial Plinian eruptions. The unprecedented observations following the Hunga 2022 eruption could be considered an isolated case. However, our observations imply that many explosive eruptions injecting water vapor and aerosols to high levels of the stratosphere are submarine (e.g., Hunga 2022, Santorini 1470 BC. and Kolumbo 1650 CE eruptions), or involving large-scale pyroclastic density current (PDC) entry into water or collapse to submarine calderas (e.g., Krakatau 1883 and Tambora 1815 eruptions). In addition, other phreatomagmatic and moderate Surtseyan eruptions can regularly inject volcanic clouds up to the stratosphere due to the high buoyancy of low-ash content and water-vapor rich plumes (e.g., Cahalan and Dufek, 2021). We show that seawater and sea salt formation can be an important process for atmospheric chemistry and aerosol microphysics at a broad range of subaerial eruptions when lava flows or PDCs enter the sea, or when eruptions disrupt coastal-influenced groundwaters or volcanic plumes incorporate sea salts in the lower atmosphere in marine settings.

Climate impacts of subaerial eruptions are not only associated with discrete large-scale eruptions, but frequent moderate eruptions also have an impact (Solomon et al., 2011; Schmidt et al., 2012). We suggest that submarine events at all scales load the atmosphere specifically and efficiently with water vapor, aerosols, SO_2/SO_4^{2-} and halogens. Future work is needed to assess the specific impacts of sea water and salts on the climate. Future models of volcanic climatic impact, and simulations and experiments of aerosol evolution in tropospheric and stratospheric conditions, should incorporate the effect of sea salts, seawater and sea-derived volatile phases as well as the different SO_2/SO_4^{2-} budget.

Data availability statement

All data shown in this publication are available in the supplementary material.

CRediT authorship contribution statement

M. Colombier: Writing – review & editing, Writing – original draft, Validation, Resources, Methodology, Investigation, Formal analysis, Conceptualization. **M. Bonifacie:** Writing – review & editing, Methodology, Investigation. **M. Brenna:** Writing – review & editing, Resources, Investigation. **A. Burke:** Writing – review & editing, Methodology, Investigation. **C. Cimarelli:** Writing – review & editing, Resources, Investigation. **S.J. Cronin:** Writing – review & editing, Resources, Investigation. **P. Delmelle:** Writing – review & editing, Methodology, Investigation. **D.B. Dingwell:** Writing – review & editing, Investigation, Funding acquisition. **K-U. Hess:** Writing – review & editing, Resources, Investigation. **M. Huebsch:** Writing – review & editing, Resources, Investigation. **T. Kula:** Writing – review & editing, Resources, Investigation. **F. Latu'ila:** Writing – review & editing, Resources, Investigation. **Y. Lavallée:** Writing – review & editing, Resources, Investigation. **G.W. Mann:** Writing – review & editing, Resources, Investigation. **T.A. Mather:** Writing – review & editing, Resources, Investigation. **J. Paredes-Mariño:** Writing – review & editing, Resources, Investigation. **T. Plank:** Writing – review & editing, Resources, Investigation. **B. Scheu:** Writing – review & editing, Resources, Investigation. **Y-J Sun:** Methodology. **Z. Taracsák:** Writing – review & editing, Methodology, Investigation. **S. Tegtmeier:** Writing – review & editing, Resources, Investigation. **S. Thivet:** Writing – review & editing, Methodology, Investigation. **M. Toohey:** Writing – review & editing, Resources, Investigation. **I. Ukstins:** Writing – review & editing, Resources, Investigation. **J. Wu:** Writing – review & editing, Resources, Investigation.

Declaration of competing interest

The authors declare that they have no known competing financial interests or personal relationships that could have appeared to influence the work reported in this paper.

Acknowledgments

DBD and MC acknowledge the support of ERC 2018 ADV Grant 834225 (EAVESDROP). CC acknowledges the support of ERC CON Grant 864052 (VOLTA). TM and TP acknowledge funding from NSFGEO-NERC grant "Sulfur cycling in subduction" (NSF award no. OCE-1933773; NERC award NE/T010940/1). GWM acknowledges funding from NERC grant "MeteorStrat" (NE/R011222), with support also from the UK National Centre for Atmospheric Science, via long-term science programme ACSIS (NE/N018001/1). ZT acknowledges support from the Leverhulme Trust (ECF-2022-396). We are grateful to the Editor Chiara Maria Petrone, Ana S. Casas and two anonymous reviewers for their constructive comments that helped to significantly strengthen our study.

Supplementary materials

Supplementary material associated with this article can be found, in the online version, at doi:10.1016/j.epsl.2025.119690.

References

Arribas Jr, A., 1995. Characteristics of high-sulfidation epithermal deposits, and their relation to magmatic fluid. Mineral. Assoc. Can. Short Course 23, 419–454.
Ayris, P.M., Lee, A.F., Wilson, K., Kueppers, U., Dingwell, D.B., Delmelle, P., 2013. SO2 sequestration in large volcanic eruptions: High-temperature scavenging by tephra. Geochim. et Cosmo. Acta 110, 58–69. https://doi.org/10.1016/j.gca.2013.02.018.
Baron, A., Chazette, P., Khaykin, S., Payen, G., Marquestaut, N., Bègue, N., Duflot, V., 2023. Early evolution of the stratospheric aerosol plume following the 2022 Hunga Tonga-Hunga Ha'apai eruption: lidar observations from reunion (21 S, 55 E). Geophys. Res. Lett. 50 (10), e2022GL101751. https://doi.org/10.1029/2022GL101751.
Bindeman, I.N., Eiler, J.M., Wing, B.A., Farquhar, J., 2007. Rare sulfur and triple oxygen isotope geochemistry of volcanogenic sulfate aerosols. Geochim. Cosmochim. Acta 71 (9), 2326–2343. https://doi.org/10.1016/j.gca.2007.01.026.
Bond, A., Sparks, R.S.J., 1976. The minoan eruption of Santorini, Greece. J. Geol. Soc. 132 (1), 1–16. https://doi.org/10.1144/gsjgs.132.1.000.
Bonifacie, M., Charlou, J.L., Jendrzejewski, N., Agrinier, P., Donval, J.P., 2005. Chlorine isotopic compositions of high temperature hydrothermal vent fluids over ridge axes. Chem. Geol. 221 (3–4), 279–288. https://doi.org/10.1016/j.chemgeo.2005.06.008.
Burke, A., Innes, H.M., Crick, L., Anchukaitis, K.J., Byrne, M.P., Hutchison, W., Wilson, R., 2023. High sensitivity of summer temperatures to stratospheric sulfur loading from volcanoes in the Northern Hemisphere. Proc. Natl. Acad. Sci. 120 (47), e2221810120. https://doi.org/10.1073/pnas.2221810120.
Cahalan, R.C., Dufek, J., 2021. Explosive submarine eruptions: the role of condensable gas jets in underwater eruptions. J. Geophys. Res. 126 (2), e2020JB020969. https://doi.org/10.1029/2020JB020969.
Caliro, S., Chiodini, G., Avino, R., Carandente, A., Cuoco, E., Di Vito, Aiuppa, A., 2025. Escalation of caldera unrest indicated by increasing emission of isotopically light sulfur. Nature Geosci. 18 (2), 167–174. https://doi.org/10.1038/s41561-024-01632-w.
Camus, G., Vincent, P.M., 1983. Discussion of a new hypothesis for the Krakatau eruption in 1883. J. Volcanol. Geotherm. Res. 19, 167–173. https://doi.org/10.1016/0377-0273(83)90130-0.
Carey, R., Soule, S.A., Manga, M., White, J.D., McPhie, J., Wysoczanski, R., McKenzie, W., 2018. The largest deep-ocean silicic volcanic eruption of the past century. Sci. Adv. 4 (1), e1701121. https://doi.org/10.1126/sciadv.1701121.
Carn, S.A., Krotkov, N.A., Fisher, B.L., Li, C., 2022. Out of the blue: volcanic SO2 emissions during the 2021–2022 eruptions of Hunga Tonga—Hunga Ha'apai (Tonga). Front. Earth Sci. 10, 976962. https://doi.org/10.3389/feart.2022.976962.
Colombier, M., Scheu, B., Kueppers, U., Cronin, S.J., Mueller, S.B., Hess, K.U., Dingwell, D.B., 2019. In situ granulation by thermal stress during subaqueous volcanic eruptions. Geology 47 (2), 179–182. https://doi.org/10.1130/G45503.1.
Colombier, M., Scheu, B., Wadsworth, F.B., Cronin, S., Vasseur, J., Dobson, K.J., Dingwell, D.B., 2018. Vesiculation and quenching during surtseyan eruptions at Hunga Tonga-Hunga Ha'apai Volcano, Tonga. J. Geophys. Res.: Solid Earth 123 (5), 3762–3779. https://doi.org/10.1029/2017JB015357.
Colombier, M., Ukstins, I.A., Tegtmeier, S., Scheu, B., Cronin, S.J., Thivet, S., Dingwell, D.B., 2023. Atmosphere injection of sea salts during large explosive submarine volcanic eruptions. Sci. Rep. 13 (1), 14435. https://doi.org/10.1038/s41598-023-41639-8.
Cronin, J.F., 1971. Recent volcanism and the stratosphere. Science 172 (3985), 847–849. https://doi.org/10.1126/science.172.3985.847.
Delmelle, P., Bernard, A., 2015. The remarkable chemistry of sulfur in hyper-acid crater lakes: a scientific tribute to Bokuichiro Takano and Minoru Kusakabe. Volcanic Lakes. Springer Berlin Heidelberg, Berlin, Heidelberg, pp. 239–259. https://doi.org/10.1007/978-3-642-36833-2_10.
De Moor, J.M., Fischer, T.P., Sharp, Z.D., Hauri, E.H., Hilton, D.R., Atudorei, V., 2010. Sulfur isotope fractionation during the May 2003 eruption of Anatahan volcano, Mariana Islands: implications for sulfur sources and plume processes. Geochim. Cosmochim. Acta 74 (18), 5382–5397. https://doi.org/10.1016/j.gca.2010.06.027.
Edmonds, M., Oppenheimer, C., Pyle, D.M., & Herd, R.A. (2003). Rainwater and ash leachate analysis as proxies for plume chemistry at Soufriere Hills Volcano, Montserrat. https://doi.org/10.1144/GSL.SP.2003.213.01.12.
Edmonds, M., Gerlach, T.M., 2006. The airborne lava–seawater interaction plume at Kīlauea Volcano, Hawai'i. Earth Planet. Sci. Lett. 244 (1–2), 83–96. https://doi.org/10.1016/j.epsl.2006.02.005.
Eggenkamp, H.G.M., 1994. δ37Cl the geochemistry of chlorine isotopes. Geol. Ultraiectina 116, 150.
Eggenkamp, H.G.M., Bonifacie, M., Ader, M., Agrinier, P., 2016. Experimental determination of stable chlorine and bromine isotope fractionation during precipitation of salt from a saturated solution. Chem. Geol. 433, 46–56. https://doi.org/10.1016/j.chemgeo.2016.04.009.
Evan, S., Brioude, J., Rosenlof, K.H., Gao, R.S., Portmann, R.W., Zhu, Y., Read, W.G., 2023. Rapid ozone depletion after humidification of the stratosphere by the Hunga Tonga Eruption. Science 382 (6668), eadg2551. https://doi.org/10.1126/science.adg2551.
Grishin, S.Y., Belousov, A.B., Belousova, M.G., Auer, A., Kozyrev, I.A., 2021. The 2019 Explosive Eruption of Raikoke Volcanic Island, Kuriles: pyroclastic Deposits and Their Impact on the Relief and Ecosystems. J. Volcanol. Seismol. 15, 387–398. https://doi.org/10.1134/S074204632105002X.
Gupta, A.K., Bennartz, R., Fauria, K.E., Mittal, T., 2022. Eruption chronology of the December 2021 to January 2022 Hunga Tonga-Hunga Ha'apai eruption sequence. Commun. Earth Environ. 3 (1), 314. https://doi.org/10.1038/s43247-022-00606-3.
Ichihara, M., Mininni, P.D., Ravichandran, S., Cimarelli, C., Vagasky, C., 2023. Multiphase turbulent flow explains lightning rings in volcanic plumes. Commun. Earth Environ. 4, 417. https://doi.org/10.1038/s43247-023-01074-z.
Johnson, R.W., Threlfall, N.A., 2023. Return to Volcano Town: Reassessing the 1937–1943 Volcanic Eruptions At Rabaul. ANU Press.
Joshi, M.M., Jones, G.S., 2009. The climatic effects of the direct injection of water vapour into the stratosphere by large volcanic eruptions. Atmos. Chem. Phys. 9 (16), 6109–6118. https://doi.org/10.5194/acp-9-6109-2009.
Junge, C.E., Gustafson, P.E., 1957. On the distribution of sea salt over the United States and its removal by precipitation. Tellus 9 (2), 164–173. https://doi.org/10.1111/j.2153-3490.1957.tb01869.x.
Khaykin, S., Podglajen, A., Ploeger, F., Grooß, J.U., Tencé, F., Bekki, S., Ravetta, F., 2022. Global perturbation of stratospheric water and aerosol burden by Hunga eruption. Commun. Earth Environ. 3 (1), 316. https://doi.org/10.1038/s43247-022-00652-x.
Kloss, C., Sellitto, P., Renard, J.B., Baron, A., Bègue, N., Legras, B., Jegou, F., 2022. Aerosol characterization of the stratospheric plume from the volcanic eruption at Hunga Tonga 15 January 2022. Geophys. Res. Lett. 49 (16), e2022GL099394. https://doi.org/10.1029/2022GL099394.
Krüger, K., Kutterolf, S., Hansteen, T.H., 2015. Halogen Release from Plinian Eruptions and Depletion of Stratospheric Ozone. Cambridge Univ. Press.
Kusakabe, M., Komoda, Y., Takano, B., Abiko, T., 2000. Sulfur isotopic effects in the disproportionation reaction of sulfur dioxide in hydrothermal fluids: implications for the δ34S variations of dissolved bisulfate and elemental sulfur from active crater lakes. J. Volcanol. Geotherm. Res. 97 (1–4), 287–307. https://doi.org/10.1016/S0377-0273(99)00161-4.
Le Glas, E., Bonifacie, M., Moretti, R., Robert, V., Agrinier, P., Labidi, J., Inostroza, M., 2025. Progressive drying of the hydrothermal system of La Soufrière de Guadeloupe (French West Indies) revealed by multi-year monitoring of chlorine isotopic composition of fumarolic HCl. J. Volcanol. Geotherm. Res., 108306 https://doi.org/10.1016/j.jvolgeores.2025.108306.
Legras, B., Duchamp, C., Sellitto, P., Podglajen, A., Carboni, E., Siddans, R., Ploeger, F., 2022. The evolution and dynamics of the Hunga Tonga–Hunga Ha'apai sulfate aerosol plume in the stratosphere. Atmos. Chem. Phys. 22 (22), 14957–14970. https://doi.org/10.5194/acp-22-14957-2022.
Li, Q., Qian, Y., Luo, Y., Cao, L., Zhou, H., Yang, T., Liu, W., 2023. Diffusion height and order of sulfur dioxide and bromine monoxide plumes from the Hunga Tonga–Hunga Ha'apai volcanic eruption. Remote Sens. 15 (6), 1534. https://doi.org/10.3390/rs15061534.
Maeno, F., Kaneko, T., Ichihara, M., Suzuki, Y.J., Yasuda, A., Nishida, K., Ohminato, T., 2022. Seawater-magma interactions sustained the high column during the 2021 phreatomagmatic eruption of Fukutoku-Oka-no-Ba. Commun. Earth Environ. 3 (1), 260. https://doi.org/10.1038/s43247-022-00594-4.
Mandeville, C.W., Sasaki, A., Saito, G., Faure, K., King, R., Hauri, E., 1998. Open-system degassing of sulfur from Krakatau 1883 magma. Earth Planet. Sci. Lett. 160, 709–722. https://doi.org/10.1016/S0012-821X(98)00122-8.
Marini, L., Moretti, R., Accornero, M., 2011. Sulfur isotopes in magmatic-hydrothermal systems, melts, and magmas. Rev. Mineral. Geochem. 73 (1), 423–492. https://doi.org/10.2138/rmg.2011.73.14.
Marshall, L.R., Maters, E.C., Schmidt, A., Timmreck, C., Robock, A., Toohey, M., 2022. Volcanic effects on climate: recent advances and future avenues. Bull. Volcanol. 84 (5), 54. https://doi.org/10.1007/s00445-022-01559-3.
Mason, E., Wieser, P.E., Liu, E.J., Edmonds, M., Ilyinskaya, E., Whitty, R.C., Oppenheimer, C., 2021. Volatile metal emissions from volcanic degassing and lava–seawater interactions at Kīlauea Volcano, Hawai'i. Commun. Earth Environ. 2 (1), 79. https://doi.org/10.1038/s43247-021-00145-3.

Mastin, L.G., Witter, J.B., 2000. The hazards of eruptions through lakes and seawater. J. Volcanol. Geotherm. Res. 97 (1–4), 195–214. https://doi.org/10.1016/S0377-0273(99)00174-2.

Mastin, L.G., Van Eaton, A.R., Cronin, S.J., 2024. Did steam boost the height and growth rate of the giant Hunga eruption plume? Bull. Volcanol. 86 (7), 64. https://doi.org/10.1007/s00445-024-01749-1.

Mather, T.A., 2015. Volcanoes and the environment: lessons for understanding Earth's past and future from studies of present-day volcanic emissions. J. Volcanol. Geotherm. Res. 304, 160–179. https://doi.org/10.1016/j.jvolgeores.2015.08.016.

McKee, C., Itikarai, I., Davies, H., 2018. Instrumental volcano surveillance and community awareness in the lead-up to the 1994 eruptions at Rabaul, Papua New Guinea. Obs. Volcano World 205–233.

McNutt, S.R., Williams, E.R., 2010. Volcanic lightning: global observations and constraints on source mechanisms. Bull. Volcanol. 72, 1153–1167. https://doi.org/10.1007/s00445-010-0393-4.

Millan, L., Santee, M.L., Lambert, A., Livesey, N.J., Werner, F., Schwartz, M.J., Froidevaux, L., 2022. The Hunga Tonga-Hunga Ha'apai hydration of the stratosphere. Geophys. Res. Lett. 49 (13), e2022GL099381. https://doi.org/10.1029/2022GL099381.

Mueller, S.B., Kueppers, U., Ametsbichler, J., Cimarelli, C., Merrison, J.P., Poret, M., Dingwell, D.B., 2017. Stability of volcanic ash aggregates and break-up processes. Sci. Rep. 7 (1), 7440. https://doi.org/10.1038/s41598-017-07927-w.

Murphy, D.M., Froyd, K.D., Bian, H., Brock, C.A., Dibb, J.E., DiGangi, J.P., Yu, P., 2019. The distribution of sea-salt aerosol in the global troposphere. Atmos. Chem. Phys. 19 (6), 4093–4104. https://doi.org/10.5194/acp-19-4093-2019.

Németh, K., Cronin, S.J., 2009. Phreatomagmatic volcanic hazards where rift-systems meet the sea, a study from Ambae Island, Vanuatu. J. Volcanol. Geotherm. Res. 180 (2–4), 246–258. https://doi.org/10.1016/j.jvolgeores.2008.08.011.

Oppenheimer, C., 2003. Ice core and palaeoclimatic evidence for the timing and nature of the great mid-13th century volcanic eruption. Int. J. Climatol. 23 (4), 417–426. https://doi.org/10.1002/joc.891.

Pernter, J. (1889), Der krakatau-ausbruch und seine folge-erschenungen meteorologische zeitschrift, vol. 6, 452–466, (pg 457 for altitude of Krakatau aerosol).

Prata, A.T., Folch, A., Prata, A.J., Biondi, R., Brenot, H., Cimarelli, C., Costa, A., 2020. Anak Krakatau triggers volcanic freezer in the upper troposphere. Sci. Rep. 10 (1), 3584. https://doi.org/10.1038/s41598-020-60465-w.

Robock, A., 2000. Volcanic eruptions and climate. Rev. Geophys. 38 (2), 191–219. https://doi.org/10.1029/1998RG000054.

Rose, W.I., Delene, D.J., Schneider, D.J., Bluth, G.J.S., Krueger, A.J., Sprod, I., Ernst, G. G., 1995. Ice in the 1994 Rabaul eruption cloud: implications for volcano hazard and atmospheric effects. Nature 375 (6531), 477–479. https://doi.org/10.1038/375477a0.

Rowell, C.R., Jellinek, A.M., Hajimirza, S., Aubry, T.J., 2022. External surface water influence on explosive eruption dynamics, with implications for stratospheric sulfur delivery and volcano-climate feedback. Front. Earth Sci. 10, 788294. https://doi.org/10.3389/feart.2022.788294.

Rye, R.O., 1993. The evolution of magmatic fluids in the epithermal environment; the stable isotope perspective. Econ. Geol. 88 (3), 733–752.

Santee, M.L., Lambert, A., Froidevaux, L., Manney, G.L., Schwartz, M.J., Millán, L.F., Fuller, R.A., 2023. Strong evidence of heterogeneous processing on stratospheric sulfate aerosol in the extrapolar Southern Hemisphere following the 2022 Hunga Tonga-Hunga Ha'apai eruption. J. Geophys. Res. 128 (16), e2023JD039169. https://doi.org/10.1029/2023JD039169.

Schmidt, A., Carslaw, K.S., Mann, G.W., Rap, A., Pringle, K.J., Spracklen, D.V., Forster, P. M., 2012. Importance of tropospheric volcanic aerosol for indirect radiative forcing of climate. Atmos. Chem. Phys. 12 (16), 7321–7339. https://doi.org/10.5194/acp-12-7321-2012.

Self, S., Sparks, R.S.J., 1978. Characteristics of widespread pyroclastic deposits formed by the interaction of silicic magma and water. Bull. Volcanol. 41, 196–212. https://doi.org/10.1007/BF02597223, 1978.

Self, S., Rampino, M.R., 1981. The 1883 eruption of Krakatau. Nature 293, 699–704. https://doi.org/10.1038/294699a0.

Self, S., 1992. Krakatau revisited: the course of events and interpretation of the 1883 eruption. Geojournal 28 (2), 109–121. https://doi.org/10.1007/BF00177223 np.

Sellitto, P., Podglajen, A., Belhadji, R., Boichu, M., Carboni, E., Cuesta, J., Legras, B., 2022. The unexpected radiative impact of the Hunga Tonga eruption of 15th January 2022. Commun. Earth Environ. 3 (1), 288. https://doi.org/10.1038/s43247-022-00618-z.

Sellitto, P., Siddans, R., Belhadji, R., Carboni, E., Legras, B., Podglajen, A., Kerridge, B., 2024. Observing the SO2 and sulfate aerosol plumes from the 2022 Hunga eruption with the infrared atmospheric sounding interferometer (IASI). Geophys. Res. Lett. 51 (19), e2023GL105565. https://doi.org/10.1029/2023GL105565.

Sioris, C.E., Malo, A., McLinden, C.A., D'Amours, R., 2016. Direct injection of water vapor into the stratosphere by volcanic eruptions. Geophys. Res. Lett. 43 (14), 7694–7700. https://doi.org/10.1002/2016GL069918.

Solomon, S., Daniel, J.S., Neely III, R.R., Vernier, J.P., Dutton, E.G., Thomason, L.W, 2011. The persistently variable "background" stratospheric aerosol layer and global climate change. Science 333 (6044), 866–870. https://doi.org/10.1126/science.1206027.

Taracsák, Z., Neave, D.A., Beaudry, P., Gunnarsson-Robin, J., Burgess, R., Edmonds, M., Hartley, M.E., 2021. Instrumental mass fractionation during sulfur isotope analysis by secondary ion mass spectrometry in natural and synthetic glasses. Chem. Geol. 578, 120318. https://doi.org/10.1016/j.chemgeo.2021.120318.

Thivet, S., Hess, K.U., Dingwell, D.B., Berthod, C., Gurioli, L., Di Muro, A., Komorowski, J.C., 2023. Volatiles of the active Mayotte volcanic chain: STA & EGA-MS analysis of volcanic products. Chem. Geol. 618, 121297. https://doi.org/10.1016/j.chemgeo.2022.121297.

Timmreck, C., 2012. Modeling the climatic effects of large explosive volcanic eruptions. Wiley Interdiscip. Rev. 3 (6), 545–564. https://doi.org/10.1002/wcc.192.

Ulvrova, M., Paris, R., Nomikou, P., Kelfoun, K., Leibrandt, S., Tappin, D.R., McCoy, F. W., 2016. Source of the tsunami generated by the 1650 AD eruption of Kolumbo submarine volcano (Aegean Sea, Greece). J. Volcanol. Geotherm. Res. 321, 125–139. https://doi.org/10.1016/j.jvolgeores.2016.04.034.

Van Eaton, A.R., Lapierre, J., Behnke, S.A., Vagasky, C., Schultz, C.J., Pavolonis, M., Khlopenkov, K., 2023. Lightning rings and gravity waves: insights into the giant eruption plume from Tonga's Hunga Volcano on 15 January 2022. Geophys. Res. Lett. 50 (12), e2022GL102341. https://doi.org/10.1029/2022GL102341.

Verbeek, R., 1884. The Krakatoa eruption. Nature 30, 10–15. https://doi.org/10.1038/030010a0.

Vernier, H., Quintão, D., Biazon, B., Landulfo, E., Souza, G., Santos, V.A., Vernier, J.P., 2025. Balloon observations suggesting sea salt injection into the stratosphere from Hunga Tonga-Hunga Ha'apai. EGUsphere 2025, 1–37. https://doi.org/10.5194/egusphere-2025-924.

Wexler, H., 1951. Spread of the Krakatoa volcanic dust cloud as related to the high-level circulation. Bull. Amer. Meteorol. Soc. 32 (2), 48–51. https://doi.org/10.1175/1520-0477-32.2.48.

Wright, C.J., Hindley, N.P., Alexander, M.J., Barlow, M., Hoffmann, L., Mitchell, C.N., Prata, A.J., Bouillon, M., Carstens, J., Clerbaux, C., Osprey, S., Powell, N., Randall, C. E., Yue, J., 2022. Surface-to-space atmospheric waves from Hunga Tonga–Hunga Ha'apai eruption. Nature 609, 741–746. https://doi.org/10.1038/s41586-022-05012-5.

Wu, J., Cronin, S.J., Brenna, M., Park, S.H., Pontesilli, A., Ukstins, I.A., Adams, D., Paredes-Mariño, J., Hamilton, K., Huebsch, M., González-García, D., Firth, C., White, J.D.L., Nichols, A.R.L., Plank, T., Vongsvivut, J., Klein, A., Ramos, F., Latu'ila, F., Kula, T., 2025. Low sulfur emissions from 2022 Hunga eruption due to seawater-magma interactions. Nat. Geosci. in press.

Yuen, D.A., Scruggs, M.A., Spera, F.J., Zheng, Y., Hu, H., McNutt, S.R., Tanioka, Y., 2022. Under the surface: pressure-induced planetary-scale waves, volcanic lightning, and gaseous clouds caused by the submarine eruption of Hunga Tonga-Hunga Ha'apai volcano. Earthq. Res. Adv. 2 (3), 100134. https://doi.org/10.1016/j.eqrea.2022.100134.

Zhang, J., Wang, P., Kinnison, D., Solomon, S., Guan, J., Stone, K., Zhu, Y., 2024. Stratospheric chlorine processing after the unprecedented Hunga Tonga eruption. Geophys. Res. Lett. 51 (17), e2024GL108649. https://doi.org/10.1029/2024GL108649.

Zhou, X., Dhomse, S.S., Feng, W., Mann, G., Heddell, S., Pumphrey, H., Chipperfield, M. P., 2024. Antarctic vortex dehydration in 2023 as a substantial removal pathway for Hunga Tonga-Hunga Ha'apai water vapor. Geophys. Res. Lett. 51 (8), e2023GL107630. https://doi.org/10.1029/2023GL107630.

Zhu, Y., Portmann, R.W., Kinnison, D., Toon, O.B., Millán, L., Zhang, J., Rosenlof, K.H., 2023. Stratospheric ozone depletion inside the volcanic plume shortly after the 2022 Hunga Tonga eruption. Atmos. Chem. Phys. 23 (20), 13355–13367. https://doi.org/10.5194/acp-23-13355-2023.